Laser-induced, Er^{3+} trace-sensitized red-to-blue photon avalanche up-conversion in Tm^{3+}-doped $LiKYF_5$ crystals

2005 J. Phys.: Condens. Matter 17 5137

(http://iopscience.iop.org/0953-8984/17/33/016)

INSTITUTE OF PHYSICS PUBLISHING JOURNAL OF PHYSICS: CONDENSED MATTER

J. Phys.: Condens. Matter **17** (2005) 5137–5148 doi:10.1088/0953-8984/17/33/016

Laser-induced, Er^{3+} trace-sensitized red-to-blue photon avalanche up-conversion in Tm^{3+}-doped $LiKYF_5$ crystals

J P Jouart[1], M Bouffard[1], E Boulma[1,2], M Diaf[2], E N Vojtenko[3] and N M Khaidukov[3]

[1] Laboratoire d'Energétique et d'Optique, UTAP, Université de Reims Champagne-Ardenne, BP 1039, Reims Cedex 51687, France
[2] Laboratoire de Physique des Rayonnements, Département de Physique, Université Badji Mokhtar, BP 12, 23000 Annaba, Algeria
[3] Kurnakov Institute of General and Inorganic Chemistry, 31 Leninskii Prospect, Moscow 119991, Russian Federation

E-mail: jp.jouart@univ-reims.fr

Received 9 March 2005, in final form 15 June 2005
Published 5 August 2005
Online at stacks.iop.org/JPhysCM/17/5137

Abstract

The results for a spectroscopic study demonstrating that the excited-state absorption (ESA) of Tm^{3+}:$LiKYF_5$ at 648 nm is dependent on the purity of starting materials used for synthesizing the crystal are presented. The Er^{3+}-free $LiKYF_5$ crystal doped with Tm^{3+} is transparent at 648 nm because the majority of the Tm^{3+} ions are in the ground $^3H_6$ state whatever the selective excitation intensity, whereas the Er^{3+}-contaminated crystal is semi-transparent. In the second case a small increase of the excitation intensity above a certain threshold produces an abrupt enhancement of the ESA process at 648 nm as well as the blue and the green emissions that are detected. All three processes, namely ESA corresponding to the $^3F_4(2) \rightarrow {}^1G_4(2)$ Tm^{3+} transition, the blue emission due to the $^1G_4 \rightarrow {}^3H_6$ Tm^{3+} transition and the green emission from the $^4S_{3/2}$ Er^{3+} level, are sensitized with the $Tm^{3+} \rightarrow Er^{3+} \rightarrow Tm^{3+}$ energy transfers which promote the conversion of Tm^{3+} ions from the $^1G_4$ and the $^3H_4$ states to the metastable $^3F_4$ state.

(Some figures in this article are in colour only in the electronic version)

1. Introduction

The sensitization mechanisms for the anti-Stokes fluorescence from rare-earth ion doped materials may be divided into two categories. Accordingly, the sensitization schemes in which a sensitizer ion absorbs the incident light energy and then non-radiatively transfers its energy

to an activator ion can be placed in the first category [1–4]. In the second category [5–27], a sensitizer ion itself does not absorb the excitation energy but it acts as a bridge through which a part of the energy from the initial excited state of one activator ion is preferably transferred down or up to a final metastable excited state of another activator ion of the same kind or another one. In this way, the fluorescence originating from the final metastable state is significantly enhanced at the expense of that from the initial state. The fact is that the absorption of one incident photon from the final metastable state can eventually bring the activator ion up to an upper excited state whose fluorescence will enhance also, or still better, up to the initial excited state of the activator ion that will then be in a position to recycle the energy.

The first scheme of the second category was suggested in 1980 [5], and this scheme was related to the Er^{3+}–Tm^{3+}–Er^{3+} system which had been discovered a few years earlier [6] by investigating anti-Stokes fluorescence from cadmium fluoride crystals doubly doped with Er^{3+} and Tm^{3+} under broadband excitation at two wavelengths, namely 1490 and 955 nm. Such a scheme was then confirmed in 1986 and 1990, by investigating YF_3 and $Sr_xCd_{1-x}F_2$ crystals doubly doped with Er^{3+} and Tm^{3+}, under laser excitation at 1500 nm [7, 8]. Since then, a number of various mechanisms belonging to the sensitization schemes of the second category were established in different host materials doubly and triply doped with optically active rare-earth ions, in particular for the following A–S–A systems, where A is an activator and S a sensitizer: Tm^{3+}–Yb^{3+}–Tm^{3+} [9–12], Pr^{3+}–Yb^{3+}–Pr^{3+} [13–18], Ho^{3+}–Yb^{3+}–Ho^{3+} [19, 20], Tm^{3+}–Er^{3+}–Tm^{3+} [21], Nd^{3+}–Yb^{3+}–Ho^{3+} [22, 23] and Nd^{3+}–Yb^{3+}–Tm^{3+} [24–27]. It should be noted that in all the cases certain excitation wavelengths were selected so as not to excite the sensitizer directly, and they were tuned to either a ground-state absorption (GSA) transition or an excited-state absorption (ESA) transition of the activator ion; in addition, A → S → A energy transfers in those systems were experimentally demonstrated. Besides, the physical consequences of the sensitization mechanisms of this type may be observed even when the excitation wavelength is no longer tuned to the GSA transitions of the activator ions and, in certain cases, as it is shown below, when the sensitizer ions are present as trace impurities in the host lattice.

In the present paper, the spectroscopic properties of $LiKYF_5$:Tm^{3+}, Er^{3+} crystals are discussed from the viewpoint of the $Tm^{3+} \rightarrow Er^{3+} \rightarrow Tm^{3+}$ energy transfers under excitation into the $^3F_4(2) \rightarrow {}^1G_4(2)$ Tm^{3+} transition in order to detect the sensitization effect of Er^{3+} ions on the blue Tm^{3+} emission in general and under trace Er^{3+} impurities in particular. Some spectroscopic data concerning a $LiKYF_5$ crystal doubly doped with 5.0 at.% Tm^{3+} and 0.1 at.% Er^{3+} under excitation at 648 nm have already been reported, and it has been shown that the $Tm^{3+} \rightarrow Er^{3+} \rightarrow Tm^{3+}$ energy transfers are responsible for the sensitization effect of Er^{3+} on the red-to-blue up-conversion of Tm^{3+} [21]. As in this case the Er^{3+} sensitizer is only a mediator for transferring energy between the Tm^{3+} ions and the energy transfer occurs within local Tm^{3+}–Er^{3+}–Tm^{3+} combinations formed in the host lattice, one can assume that this sensitization effect, referred to as a sensitized photon avalanche, should be still observed under a lower Er^{3+} concentration than 0.1 at.%. Accordingly, the Er^{3+} contaminant of any host could be an indispensable condition to detect up-converted emission from Tm^{3+} due to the photon avalanche process.

2. Experimental details

Low-temperature luminescence spectra were measured under 648 nm continuous wave (cw) excitation of 5.0 at.% Tm^{3+}-doped $LiKYF_5$ crystals in which trace amounts of Er^{3+} ions irregularly dispersed in the host at the concentration level lower than 10^{-3} at.% were detected. This value was estimated with measurement of the red and the green emission intensity from

Er^{3+} under direct one-step and two-step excitation, respectively. The doped $LiKYF_5$ crystals grown by the hydrothermal method [28] were excited by using a Spectra-Physics 375 tunable dye laser pumped with a cw argon-ion laser. The excitation beam, with a spectral width of the order of 10^{-2} nm, was focused within the crystal with a lens having a 30 cm focal length. Taking into account the previous study of $LiKYF_5$ crystals doubly doped with 5.0 at.% Tm^{3+} and 0.1 at.% Er^{3+} [21], the 648 nm excitation wavelength was accurately selected because the mechanisms triggered by this wavelength could be described within the framework of Er^{3+}-sensitized photon avalanche absorption.

A selective excitation technique [29] was also used to check the presence of Er^{3+} ions at different points in the crystal. The 475.5 nm [$^1G_4(1) \rightarrow {}^3H_6(1)$] blue emission from Tm^{3+} ions as well as the 656.3 nm [$^4F_{9/2}(1) \rightarrow {}^4I_{15/2}(3)$] red and the 542.4 nm [$^4S_{3/2}(2) \rightarrow {}^4I_{15/2}(3)$] green emissions from Er^{3+} ions were selected by a Coderg three-grating spectrometer and detected by a cooled photomultiplier (EMI 9558 QB). The 1860 nm [$^3F_4 \rightarrow {}^3H_6$] infrared fluorescence from Tm^{3+} ions was selected by a Jobin-Yvon M25 monochromator and detected by a PbS photoresistance associated with a PAR 121 lock-in amplifier. Excitation spectra were recorded in the spectral regions from 625 to 660 nm for the $^3F_4 \rightarrow {}^1G_4$, the $^3H_4 \rightarrow {}^1D_2$ and the $^3H_6 \rightarrow {}^3F_2$ transitions in the Tm^{3+} ions and from 633 to 660 nm for the $^4I_{13/2} \rightarrow {}^4F_{5/2}$ and the $^4I_{15/2} \rightarrow {}^4F_{9/2}$ transitions in the Er^{3+} ions. As the excitation power varies only 20% in the spectral range we probed, the excitation spectra have not been corrected.

Some other samples, namely $LiKYF_5$:0.1 at.% Tm^{3+}, $LiKYF_5$:0.1 at.% Er^{3+}, 5.0 at.% Tm^{3+} and $LiKYF_5$:1.0 at.% Er^{3+}, 5.0 at.% Tm^{3+}, were also investigated in order to contrast spectroscopic properties of the crystals containing different concentrations of the optically active rare-earth ions. All the measurements were performed at liquid nitrogen temperature.

For the decay-time and rise-time measurements, the laser beam was turned off and on by an electro-optic modulator, and an oscillograph interfaced with a microcomputer was used to record the decay and rise of luminescence.

3. Results and discussion

3.1. Excitation spectra of Tm^{3+} emissions from $^3F_4$ and $^1G_4$

The excitation spectrum within the spectral range of the GSA $^3H_6 \rightarrow {}^3F_2$ transition for the Tm^{3+} ($^3F_4$) emission from $LiKYF_5$:5.0 at.% Tm^{3+} is presented in figure 1. This spectrum is comprised of three peaks (660, 658.2 and 656.25 nm) attributed to transitions coming from first Stark level of the Tm^{3+} ($^3H_6$) ground state and going to three of five Stark levels of $^3F_2$ that we locate at 15 152, 15 193 and 15 238 cm^{-1}. The excitation spectrum for the Tm^{3+} ($^1G_4$) blue emission is completely different: the main lines of this spectrum correspond to the ESA $^3F_4 \rightarrow {}^1G_4$ transition, while the lines corresponding to the GSA $^3H_6 \rightarrow {}^3F_2$ transition are extremely weak. Figure 2 shows the excitation spectra of the Tm^{3+} ($^1G_4$) emission for $LiKYF_5$:0.1 at.% Tm^{3+} and $LiKYF_5$:5.0 at.% Tm^{3+}, 0.1 at.% Er^{3+} in the range of the ESA $^3F_4 \rightarrow {}^1G_4$ transition. At low concentrations ($\leqslant$0.1 at.%) of Tm^{3+} ions, the blue-emitting $^1G_4$ level is populated through a two-step absorption process via the metastable $^3F_4$ level [30]. Under these conditions, the blue-emission intensity from Tm^{3+} ions is proportional to the product of the absorption cross-sections on either step. As the absorption cross-section of the first step ($^3H_6 \rightarrow {}^3F_2$) hardly varies for wavelengths shorter than 655 nm, the spectrum (a) of figure 2 mainly represents the variation of the absorption cross-section of the second step ($^3F_4 \rightarrow {}^1G_4$). As most Tm^{3+} ions are well separated from each other in $LiKYF_5$:0.1 at.% Tm^{3+}, there is no quenching of the blue emission in this sample while the blue emission from $LiKYF_5$:5.0 at.% Tm^{3+} is totally quenched at 648 nm in the Er^{3+}-free regions, as one can see in

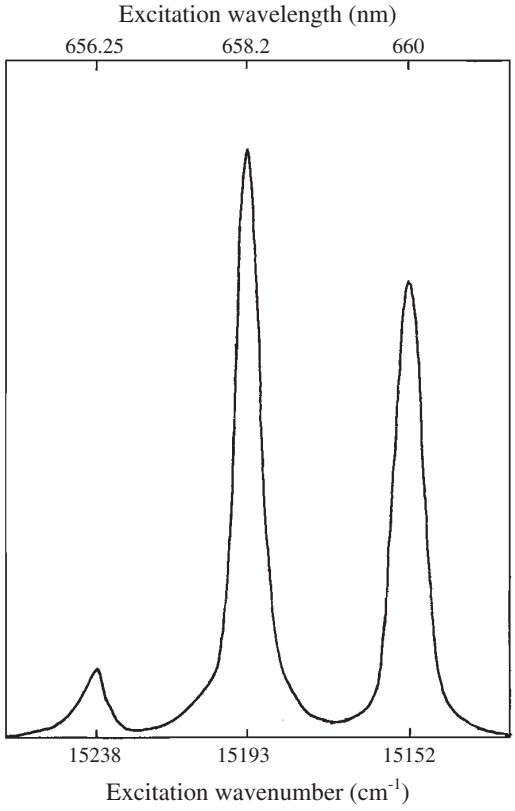

Figure 1. Excitation spectrum of $LiKYF_5$:5.0 at.% Tm^{3+} for the spectral range of the GSA $^3H_6 \rightarrow {}^3F_2$ transition obtained by monitoring the Tm^{3+} $^3F_4 \rightarrow {}^3H_6$ emission at 1860 nm.

figure 7. It will be noted that the quenching of the blue emission is due to non-resonant energy transfers of cross-relaxation type between an excited Tm^{3+} ion and one nearby unexcited Tm^{3+} ion [31, 32].

3.2. Excitation spectra of Er^{3+} emissions from $^4F_{9/2}$ and $^4S_{3/2}$

Part of the excitation spectrum in the range of the GSA $^4I_{15/2} \rightarrow {}^4F_{9/2}$ transition for the Er^{3+} ($^4F_{9/2}$) emission from $LiKYF_5$:1.0 at.% Er^{3+}, 5.0 at.% Tm^{3+} is shown in figure 3, and as one can see from the figure, no Er^{3+} GSA peak is detected at 648 nm. On the other hand, figure 4 presents the excitation spectrum of the Er^{3+} ($^4S_{3/2}$) emission for $LiKYF_5$:5.0 at.% Tm^{3+}, 0.1 at.% Er^{3+} in the range of the ESA $^4I_{13/2} \rightarrow {}^4F_{5/2}$ transition. For these excitation wavelengths the green-emitting $^4S_{3/2}$ level of Er^{3+} ions is populated through a two-step absorption process via the metastable $^4I_{13/2}$ level [29]. As the absorption cross-section of the first step ($^4I_{15/2} \rightarrow {}^4F_{9/2}$) hardly varies for wavelengths shorter than 640 nm, the spectrum in the figure 4 mainly illustrates the variation of the absorption cross-section for the second step, namely the $^4I_{13/2} \rightarrow {}^4F_{5/2}$ transition.

3.3. Sensitized photon avalanche mechanism for the Tm^{3+}, Er^{3+} system

Under laser excitation at 648 nm, the 1860 nm infrared fluorescence due to the $^3F_4 \rightarrow {}^3H_6$ Tm^{3+} transition in $LiKYF_5$:5.0 at.% Tm^{3+} is sensitized with a trace amount of Er^{3+} ions whose

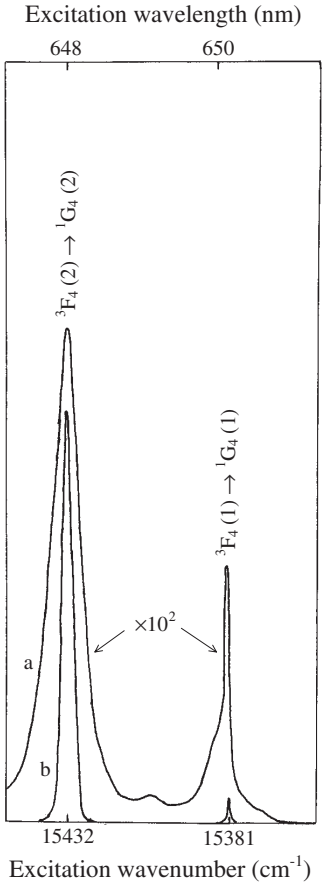

Figure 2. Excitation spectrum in the 647.25–651.5 nm spectral range for the ESA process from the $^3F_4$ Tm^{3+} state obtained by the $^1G_4(1) \rightarrow {}^3H_6(1)$ Tm^{3+} emission at 475.5 nm for $LiKYF_5$:0.1 at.% Tm^{3+} (a) and $LiKYF_5$:5.0 at.% Tm^{3+}, 0.1 at.% Er^{3+} (b).

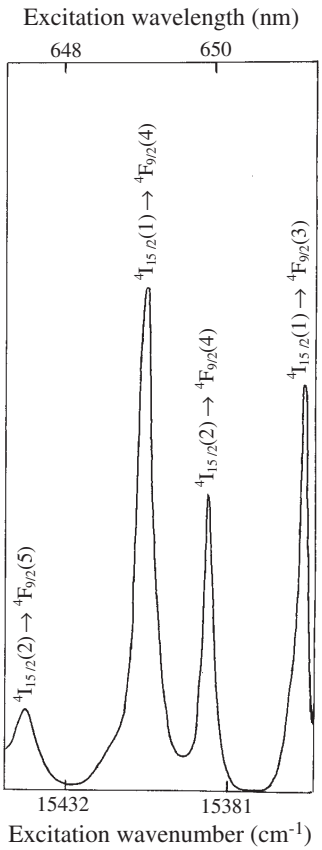

Figure 3. Excitation spectrum of Er^{3+}:$LiKYF_5$ in the 647.25–651.5 nm spectral range for the $^4F_{9/2}(1) \rightarrow {}^4I_{15/2}(3)Er^{3+}$ emission at 656.3 nm.

$^4I_{15/2} \rightarrow {}^4I_{13/2}$ transition is in resonance with the $^1G_4 \rightarrow {}^3F_3$ and $^3H_4 \rightarrow {}^3F_4$ transitions of Tm^{3+} ions [21]. Thus, the Er^{3+} ions increase the possibilities of resonant energy transfers between Tm^{3+} ions, and consequently, the excitation probability of Tm^{3+} ions into the $^3F_4$ state. As the probability of a resonant energy transfer is much higher than that of a non-resonant one [33], accordingly the excitation energy is transferred via the $Tm^{3+} \rightarrow Er^{3+} \rightarrow Tm^{3+}$ pathway in preference to the direct one. In this case, a part of the energy initially absorbed by the Tm^{3+} ions is resonantly transferred from the $^1G_4$ and $^3H_4$ levels of the Tm^{3+} ions to the $^4I_{13/2}Er^{3+}$ level, and then there is the energy transfer from the $^4I_{13/2}Er^{3+}$ level to the $^3F_4$ Tm^{3+} level [34–36] from which the Tm^{3+} ions are again excited up to the $^1G_4$ state through the strong ESA process, which causes the recycling of the energy eventually (see figure 5). In reality, the spectral width of the laser excitation wavelength is not sufficiently broad that all the Tm^{3+} ions could be re-excited to the $^1G_4$ state. The fact is that the Tm^{3+} ions can be excited with the laser beam only into the $^3F_4(2) \rightarrow {}^1G_4(2)$ inter-Stark transition which is in resonance with

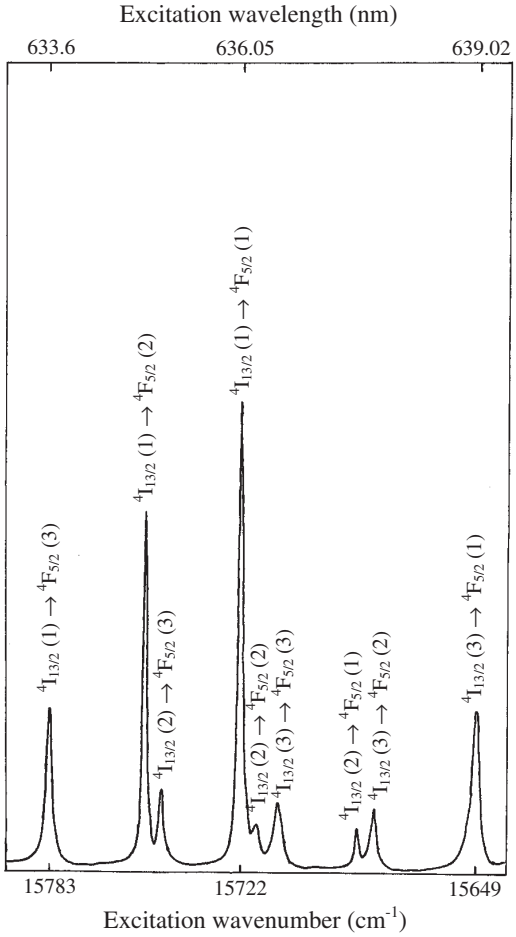

Figure 4. Excitation spectrum in the spectral range of the ESA $^4I_{13/2} \rightarrow {}^4F_{5/2}$ Er^{3+} transition for the $^4S_{3/2}(2) \rightarrow {}^4I_{15/2}(3)$ Er^{3+} emission from $LiKYF_5$:5.0 at.% Tm^{3+}, 0.1 at.% Er^{3+} at 542.4 nm.

its wavelength. Obviously, in this case far more of the $^3F_4$ than of the $^1G_4$ excited Tm^{3+} ions are formed. However, it will be noted that the intensity of the 1860 nm infrared fluorescence generated by the excitation wavelength of 648 nm is about 20 times less than that of the infrared fluorescence which is excited with the 658.2 nm excitation wavelength tuned to the $^3H_6(1) \rightarrow {}^3F_2(2)$ transition of the Tm^{3+} ion. Seemingly, the Tm^{3+} ions which are located close to the Er^{3+} ions and, accordingly, which can be excited under the 648 nm wavelength, represent only a very small fraction of the whole Tm^{3+} concentration in the $LiKYF_5$ crystal. In this context, the Er^{3+} ions are not only able to excite all the Tm^{3+} ions located around them through energy transfer but can also maintain the Tm^{3+} ions in their $^3F_4$ metastable state. The Er^{3+} ion released by the $Er^{3+} \rightarrow Tm^{3+}$ transfer is immediately re-excited in the $^4I_{13/2}$ state by the $Tm^{3+} \rightarrow Er^{3+}$ transfer. In order that the Er^{3+} ions could be operative, that is to say, in order that they could transfer the excitation energy from one Tm^{3+} ion to an other one, it is necessary that the Er^{3+} absorption at 648 nm would be very weak, which is indeed the case. On the other hand, the number of Tm^{3+} ions excited to the metastable $^3F_4$ state increases as a function of the excitation intensity until all the Er^{3+} ions are involved in the avalanche effect.

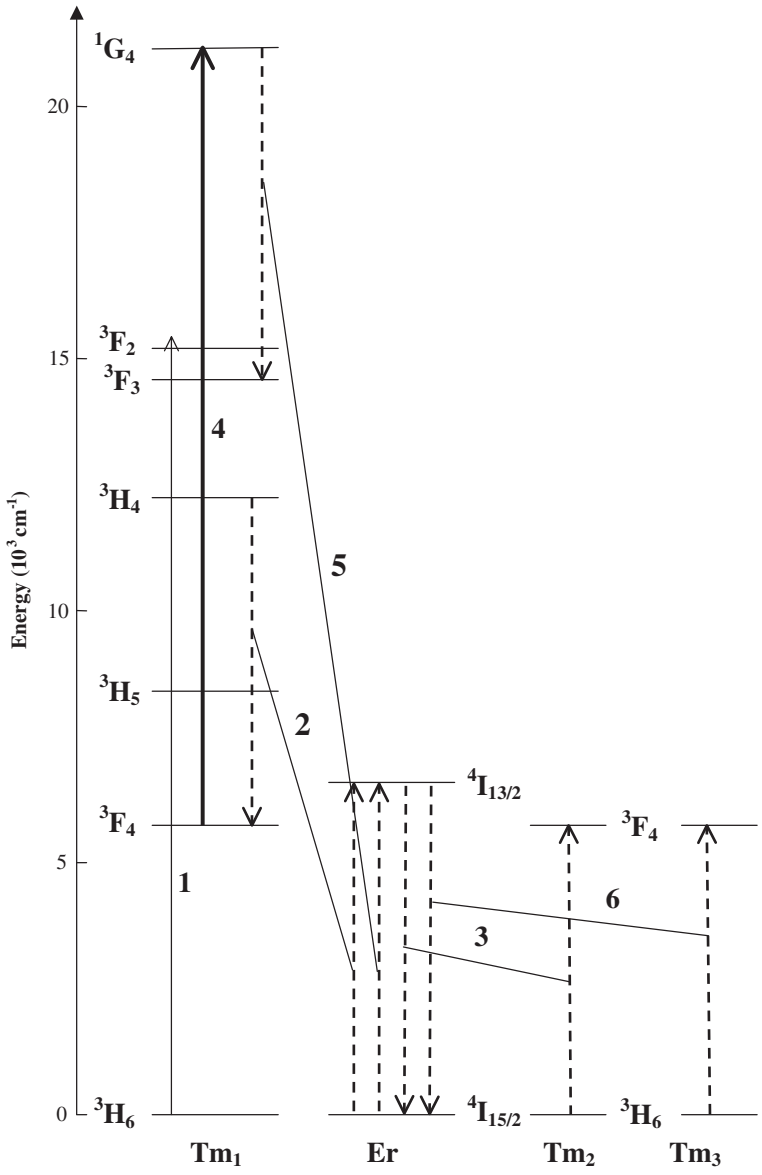

Figure 5. Energy level diagram explaining the sensitized photon avalanche mechanism for the Tm^{3+}, Er^{3+} system in $LiKYF_5$ excited at 648 nm: 1—ground-state absorption (GSA); 2 and 5—$Tm^{3+} \rightarrow Er^{3+}$ resonant energy transfer processes; 4—excited-state absorption (ESA); 3 and 6—$Er^{3+} \rightarrow Tm^{3+}$ energy transfer processes.

When all the Tm^{3+} ions are in the $^3F_4$ metastable state, there are no cross-relaxation processes and, accordingly, there is no self-quenching. Thus, if the excitation wavelength is resonantly tuned to the ESA $^3F_4(2) \rightarrow {}^1G_4(2)$ transition of the Tm^{3+} ion at 648 nm, green emission arises from Er^{3+} ions excited by ESA from the $^4I_{13/2}$ level. These Er^{3+} ions are surrounded by Tm^{3+} ions excited in the $^3F_4$ state by the energy transfer Er^{3+} ($^4I_{13/2}$) $\rightarrow Tm^{3+}$ and, therefore, the Er^{3+} ions do not undergo the quenching effects due to energy transfers from Er^{3+} ($^4S_{3/2}$) to Tm^{3+} [5]. Obviously, the overpopulation of the $^4I_{13/2}$ and the $^4S_{3/2}$ Er^{3+} levels is due to

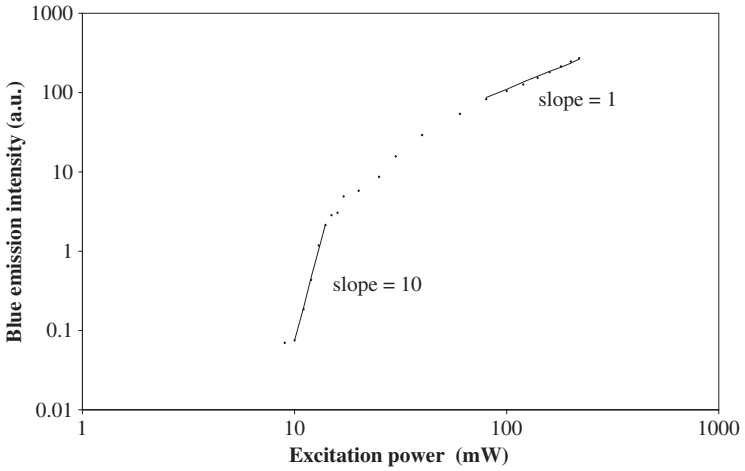

Figure 6. Dependence of the blue (475.5 nm) emission intensity on the 648 nm laser excitation power delivered into an Er^{3+}-contaminated zone of $LiKYF_5$:5.0 at.% Tm^{3+}.

the sensitized photon avalanche mechanism (figure 5). It should be noted that the efficiency of this mechanism is two orders of magnitude higher than that of the sequential two-photon absorption process populating the green-emitting $^4S_{3/2}$ level when the excitation wavelength is in resonance with the ESA $^4I_{13/2}(1) \rightarrow {}^4F_{5/2}(1)$ transition of the Er^{3+} ion at 636.05 nm. On the excitation spectrum of the Er^{3+} ($^4S_{3/2}$) green emission from Er^{3+}-contaminated regions of $LiKYF_5$:5.0 at.% Tm^{3+} recorded between 633 and 653 nm (this spectrum is not presented), we can indeed see that the intensity of the Tm^{3+} line located at 648 nm is two orders of magnitude higher than that of the Er^{3+} line located at 636.05 nm. This difference in efficiency is mainly due to a difference in $^4I_{13/2}$ population between the two ways of excitation. Under direct excitation at 636.05 nm, the Er^{3+} ($^4I_{13/2}$) and Er^{3+} ($^4S_{3/2}$) populations are extremely weak because of quenching effects due to Tm^{3+} ($^3H_6$) ions. Under 648 nm, the excitation of the $^4I_{13/2}$ level takes place via the resonant transfer Tm^{3+} ($^1G_4$) $\rightarrow$ Er^{3+}; the $^4I_{13/2}$ population is then much higher than under 636.05 nm. Although 648 nm is slightly detuned in comparison with the ESA $^4I_{13/2} \rightarrow {}^4F_{5/2}$ transition, the $^4S_{3/2}$ population is also much higher than under 636.05 nm because of sensitization effects due to $Tm^{3+}[^3F_4(2)]$ ions.

3.4. Properties of Tm^{3+} blue emission from an Er^{3+}-contaminated zone of $LiKYF_5$:5.0 at.% Tm^{3+}

The blue emission is generated by the Tm^{3+} ions that reach the $^1G_4$ level and are not under the influence of cross-relaxations. These ions are excited to the $^1G_4$ level through ESA from the metastable $^3F_4$ state whose population first grows with the excitation intensity and then stabilizes at a constant level dependent on the Er^{3+} ion concentration. The linear dependence of the blue fluorescence intensity that is observed after the steep rise (figure 6), which characterizes the avalanche effect, agrees with this interpretation. Though the spatial distribution of non-excited Tm^{3+} ions is fairly uniform within the samples, important variations of the local excitation density are observed for the blue $^1G_4 \rightarrow {}^3H_6$ emission whose intensity is highly sensitive to the local concentration of Er^{3+} ions which are present as trace impurities within the host lattice. In particular, no blue emission is detected in the Er^{3+}-free regions, whereas a strong blue emission arising from Tm^{3+} ions located in the Er^{3+}-contaminated regions clearly

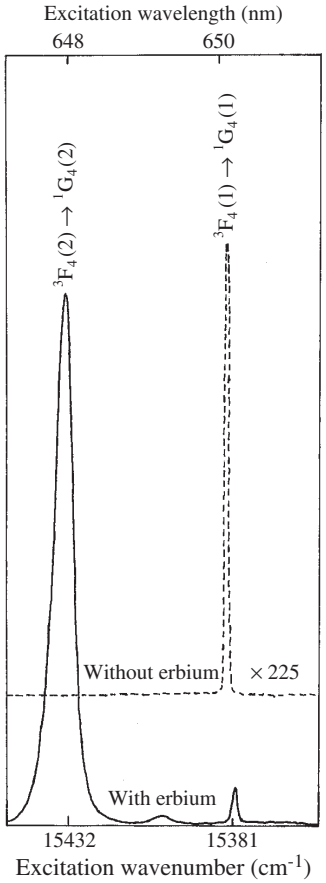

Figure 7. Excitation spectra of the blue (475.5 nm) emission from an Er^{3+}-contaminated zone (full curve) and an Er^{3+}-free zone (broken curve) in $LiKYF_5$:5.0 at.% Tm^{3+}.

develops (see figure 7). It should be emphasized that in the Er^{3+}-contaminated regions, the ground $^3H_6$ Tm^{3+} state population decreases when the excitation intensity increases. Besides, under high excitation intensities, most of the Tm^{3+} ions are in the metastable state, with the result that the cross-relaxation processes are suppressed. On the other hand, in the Er^{3+}-free regions, most of the Tm^{3+} ions remain in the ground state and, accordingly, the cross-relaxation processes can function as well as the $^1G_4$ emission being totally quenched. Most of the Tm^{3+} ions excited to the metastable $^3F_4$ state thanks to the sensitized avalanche effect (figure 5) exist round the Er^{3+} ions heterogeneously distributed in the crystal and, as a result, in the crystal there are blue-emitting spots within which the excitation is self-confined. It is supposed that the Er^{3+} ions are sufficiently separated not to interact but are also near enough to the Tm^{3+} ions localized round them in order to maintain the metastable $^3F_4$ state of the Tm^{3+} ions. Depending on the incident energy density, the avalanche effect spreads more or less deeply over the whole of the Er^{3+}-contaminated zones excited by the laser beam. Considering that the interaction between two neighbouring Tm^{3+} ions excited to the $^3F_4$ state is negligible, the Er^{3+} traces, which could be inevitably introduced in consequence of the doping with the Tm^{3+} ions or some other sources, might be the feasible cause of the photon avalanche effect that has been observed in most Tm^{3+}-doped materials [37].

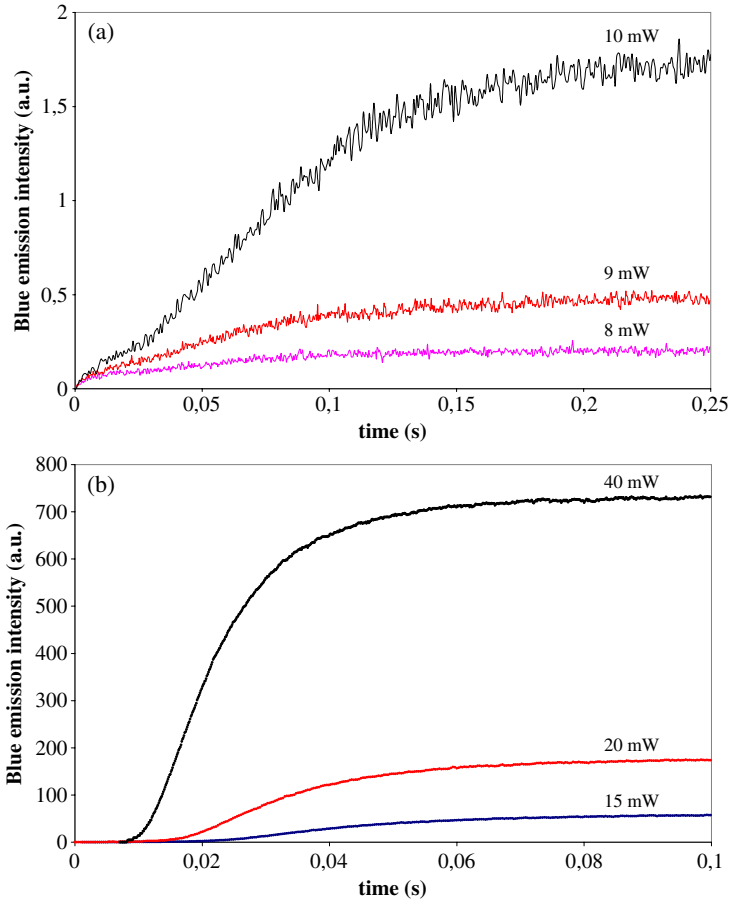

Figure 8. Excitation power-dependent build-up of the blue (475.5 nm) emission resulting from the photon avalanche absorption at 648 nm in an Er^{3+}-contaminated zone of $LiKYF_5$:5.0 at.% Tm^{3+} near (a) and above (b) the avalanche threshold. The excitation power is given above each rise curve. The blue emission is not detectable from 7 mW.

The study of the blue emission build-up (figures 8(a) and (b)) confirms that the up-conversion mechanism is definitely the photon avalanche. Near the avalanche threshold, we note that the blue emission rise-time (about 200 ms at 10 mW on figure 8(a)) is longer than the lifetime of the $^3F_4$ reservoir level and that the rise-time increases with the excitation power. Above the avalanche threshold, an inflexion point appears on the rise curve that becomes faster as the excitation power increases (figure 8(b)).

Figure 9 shows that the decay of the infrared emission at 1860 nm ($^3F_4 \rightarrow {}^3H_6$) is not exponential because the energy transfers continue to populate $^3F_4$ after the cut-off of the laser beam. At the end of the decay, when the energy transfers no longer have any effect, the decay becomes exponential with a time constant of about 2.7 ms for $LiKYF_5$:5.0 at.% Tm^{3+}.

4. Conclusion

The inhomogeneous distribution of excited Tm^{3+} ions has been generated and detected in Tm^{3+}: $LiKYF_5$ under continuous wave laser excitation at a wavelength of 648 nm. It has turned

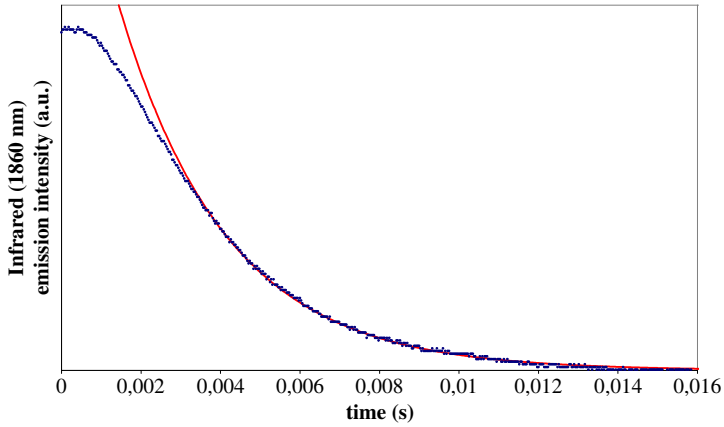

Figure 9. Infrared (1860 nm) emission decay after ESA excitation at 648 nm in an Er^{3+}-contaminated zone of $LiKYF_5$:5.0 at.% Tm^{3+}. The end of the decay has been fitted by an exponential (continuous line) whose time constant is 2.7 ms.

out that these inhomogeneities are due to Er^{3+} ions present as local trace impurities whose number is quite sufficient to trigger an avalanche effect amongst the Tm^{3+} ions localized in the Er^{3+}-contaminated regions of the host lattice. It has been discovered that the ESA process corresponding to the $^3F_4(2) \rightarrow {}^1G_4(2)$ transition, the blue emission from Tm^{3+} ions and the green emission from Er^{3+} ions are sensitized by the $Tm^{3+} \rightarrow Er^{3+} \rightarrow Tm^{3+}$ energy transfer processes that encourage the conversion of Tm^{3+} ions from the $^1G_4$ and the $^3H_4$ states to the metastable $^3F_4$ state.

References

[1] Auzel F 1966 *C. R. Acad. Sci.* **263** 819
[2] Esterowitz L, Noonan J and Bahler J 1967 *Appl. Phys. Lett.* **10** 126
[3] Feofilov P P and Ovsyankin V V 1967 *Appl. Opt.* **6** 1828
[4] Thrash R J and Johnson L F 1994 *J. Opt. Soc. Am.* B **11** 881
[5] Jouart J P 1980 *J. Lumin.* **21** 153
[6] Jouart J P 1977 *Thèse d'Etat* Reims
[7] Van der Ziel J P, Van Uitert L G, Grodkiewicz W H and Mikulyak R M 1986 *J. Appl. Phys.* **60** 4262
[8] Jouart J P and Mary G 1990 *J. Lumin.* **46** 39
[9] Wu Xu, Denis J P, Özen G, Goldner Ph, Genotelle M and Pellé F 1993 *Chem. Phys. Lett.* **203** 211
[10] Zhang X X, Hong P, Bass M and Chai B H T 1995 *Phys. Rev.* B **51** 9298
[11] Martin I R, Méndez-Ramos J, Rodriguez V D, Romero J J and Garcia-Solé J 2003 *Opt. Mater.* **22** 327
[12] Lahoz F, Martin I R, Méndez-Ramos J and Nunez P 2004 *J. Chem. Phys.* **120** 6180
[13] Gosnell T R 1997 *Electron. Lett.* **33** 411
[14] Sandrock T, Scheife H, Heumann E and Huber G 1997 *Opt. Lett.* **22** 808
[15] Lupei V, Osiac E, Sandrock T, Heumann E and Huber G 1998 *J. Lumin.* **76/77** 441
[16] Zellmer H, Riedel P and Tünnermann A 1999 *Appl. Phys.* B **69** 417
[17] Osiac E, Heumann E, Huber G, Kück S, Sani E, Toncelli A and Tonelli M 2003 *Appl. Phys. Lett.* **82** 3832
[18] Osiac E, Kück S, Heumann E, Huber G, Sani E, Toncelli A and Tonelli M 2003 *Opt. Mater.* **24** 537
[19] Zhang X, Jouart J P and Mary G 1998 *J. Phys.: Condens. Matter* **10** 493
[20] Lahoz F, Martin I R and Briones A 2004 *J. Appl. Phys.* **95** 2957
[21] Jouart J P, Bouffard M, Duvaut T and Khaidukov N M 2002 *Chem. Phys. Lett.* **366** 62
[22] Qiu J, Shojiya M and Kawamoto Y 1999 *J. Appl. Phys.* **86** 909
[23] Qiu J, Kawamoto Y and Zhang J 2002 *J. Appl. Phys.* **92** 5163
[24] Qiu J and Kawamoto Y 2001 *J. Fluorine Chem.* **110** 175

[25] Qiu J and Kawamoto Y 2002 *J. Appl. Phys.* **91** 954
[26] Qiu J, Mukai A, Makishima A and Kawamoto Y 2002 *J. Phys.: Condens. Matter* **14** 13827
[27] Gouveia-Neto A S, da Costa E B, dos Santos P V, Bueno L A and Ribeiro S J L 2003 *J. Appl. Phys.* **94** 5678
[28] Balda R, Fernandez J, Saez de Ocariz I, Voda M, Garcia A J and Khaidukov N M 1999 *Phys. Rev.* B **59** 9972
[29] Jouart J P, Bissieux C and Mary G 1987 *J. Phys. C: Solid State Phys.* **20** 2019
[30] Bouffard M, Jouart J P and Joubert M F 2000 *Opt. Mater.* **14** 73
[31] Van Uitert L G and Johnson L F 1966 *J. Chem. Phys.* **44** 3514
[32] Oomen E W J L 1992 *J. Lumin.* **50** 317
[33] Miyakawa T and Dexter D L 1970 *Phys. Rev.* B **31** 2961
[34] Johnson L F, Van Uitert L G, Rubin J J and Thomas R A 1964 *Phys. Rev.* **133** A494
[35] Voron'ko Yu K, Dmitruk M V, Osiko V V and Udovenchik V T 1968 *Sov. Phys.—JETP* **27** 197
[36] Brenier A, Moncorgé R and Pedrini C 1990 *IEEE J. Quantum Electron.* **26** 967
[37] Hebert T, Wannemacher R, Macfarlane R M and Lenth W 1992 *Appl. Phys. Lett.* **60** 2592